

# Synthesis, Characterization and Optical Activity of RE-doped ZnWO<sub>4</sub> Nanorods and Nanospheres by Hydrothermal Method

Kellen Cristina Mesquita Borges<sup>\*a</sup>, Rosana de Fátima Gonçalves<sup>a,b</sup>, Murillo Henrique de Matos Rodrigues<sup>a</sup>, Rívia Aparecida Reinalda Arruda<sup>a</sup>, Maria Rita de Cassia Santos<sup>a</sup>, Ana Paula Azevedo Marques<sup>b</sup>, and Mario Godinho Júnior<sup>a</sup>

<sup>a</sup>UFG- Universidade Federal de Goiás, Regional Catalão, Av. Lamartine, Catalão, GO, Brazil

<sup>b</sup>UNIFESP- Universidade Federal de São Paulo, Rua Prof. Artur Riedel, 275, Diadema, SP, Brazil

*Article history:* Received: 28 October 2018; revised: 16 February 2019; accepted: 19 February 2019. Available online: 14 April 2019. DOI: <http://dx.doi.org/10.17807/orbital.v11i2.1350>

## Abstract:

This work has investigated the effect of different dopants on structure, morphology and optical property of ZnWO<sub>4</sub>. Rare-earth doped ZnWO<sub>4</sub> (ZnWO<sub>4</sub>:RE, with 0.5, 1, and 2 mol% of Eu<sup>3+</sup> and Pr<sup>3+</sup>) were successfully synthesized by coprecipitation method followed by microwave-assisted hydrothermal system at 140 °C for 1 h. XRD indicated that the crystals have a wolframite- type monoclinic structure and with the addition of dopants the crystallite size decreased. HR-TEM images revealed interesting homogenous nanorods for pure ZnWO<sub>4</sub> crystals with grow along (021) direction. For ZnWO<sub>4</sub>: RE we have found nanospheres morphologies, in which the decreasing crystal size were dependent on the RE doping concentration. IR spectra confirm the crystals structure. Ultraviolet-Visible diffuse reflectance spectra indicated that the optical band gap varies with increasing replacement of Zn<sup>2+</sup> by RE ions. E<sub>gap</sub> was characteristic of semiconductor materials.

**Keywords:** microwave- hydrothermal method; nanomaterials; rare earth; semiconductor

## 1. Introduction

Metal tungstates have attracted much attention due to their important applications as photoluminescent materials [1-3], microwave applications [4, 5], sensors [6], optical devices [7], photocatalysts [8], supercapacitors [9, 10] and others [11, 12]. Among of them, zinc tungstate (ZnWO<sub>4</sub>) has shown prominence due its interesting in chemical and physical properties, strongly influenced by particle size, chemical composition, addition of dopants and surface chemistry [13].

Doping strategy via chemistry solution using coprecipitation followed by microwave hydrothermal method (MWH) may provide well-controlled ways to modify the structures, morphologies, particle sizes, and surface features by means of adaptation on the compositions of the crystals [2, 8, 14, 15].

Therefore, the incorporation of the rare earth ions on the pure ZnWO<sub>4</sub> such as Eu<sup>3+</sup> and Pr<sup>3+</sup> ions replacing the Zn<sup>2+</sup> site can result in changes on sizes and shapes of pure ZnWO<sub>4</sub> particles, as well as can to improve their property [14-17].

## 2. Results and Discussion

Fig. 1a-b shows the XRD pattern obtained for ZnWO<sub>4</sub>: RE (RE= Eu<sup>3+</sup> and Pr<sup>3+</sup> with 0.5, 1.0 and 2.0% mol). All diffraction peaks were indexed to the wolframite-type monoclinic structure according to the standard card (ICDD Card number: 00-015-0774).

The use MWH has provided the production of crystalline materials under moderate heating conditions, in aqueous and alkaline medium, with temperatures and times significantly lower than those reported in the literature [14, 18]. Consequently, these conditions and the addition

\*Corresponding author. E-mail: [kellenquim@gmail.com](mailto:kellenquim@gmail.com)

of dopants contribute to the reduction of particle size. By use the Scherrer's formula from the predominant plan (111) we have obtained the mean crystallite size of  $\text{ZnWO}_4: \text{RE}^{3+}$ . The found values were 9.60 nm for pure  $\text{ZnWO}_4$  and 7.32, 5.89 and 3.62 nm for 0.5, 1.0 and 2.0 mol% of  $\text{Eu}^{3+}$ , respectively. For  $\text{ZnWO}_4$  doped with 0.5, 1.0 and 2.0 mol% of  $\text{Pr}^{3+}$  the mean crystallite size were 9.50, 3.84 and 3.10 nm, respectively.

The decrease in crystallite size occurs through defects generated by the substitution of the network modifier ( $\text{Zn}^{2+}$ ) by the dopant ( $\text{Eu}^{3+}$  or  $\text{Pr}^{3+}$ ), generating distortions in the crystalline lattice [19], which consequently contributes to technological applications.

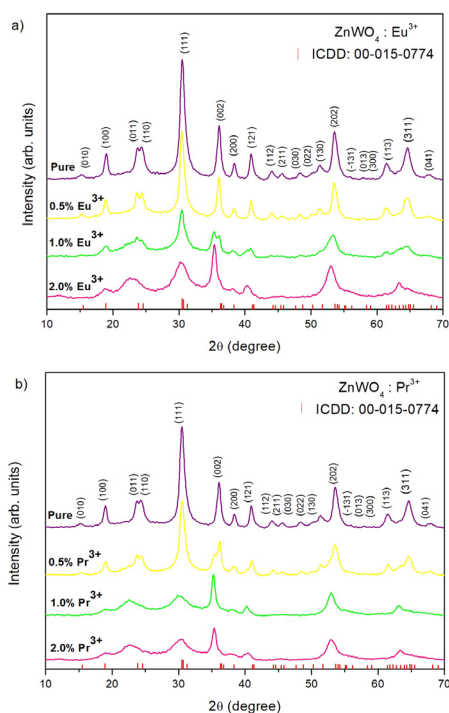


**Figure 1.** XRD patterns of: a)  $\text{Eu}^{3+}$ -doped  $\text{ZnWO}_4$  powders b)  $\text{Pr}^{3+}$ -doped  $\text{ZnWO}_4$  powders.

Optical band gap energy ( $E_{\text{gap}}$ ) values were calculated using the Kubelka–Munk equation [20]. From the extrapolation of the linear part of the curve in the Kubelka–Munk function it is possible to establish  $E_{\text{gap}}$  (Fig. 2). From this,  $E_{\text{gap}}$  values decrease with increasing dopant concentration. This is due to the presence of RE in the lattice, resulting in intermediate energy levels between valence band (VB) and conduction band (CB) and electronic energy levels related to the additional 4f orbitals of the

dopant [20]. This behavior contributes to applications in photoluminescence and photocatalysis area.

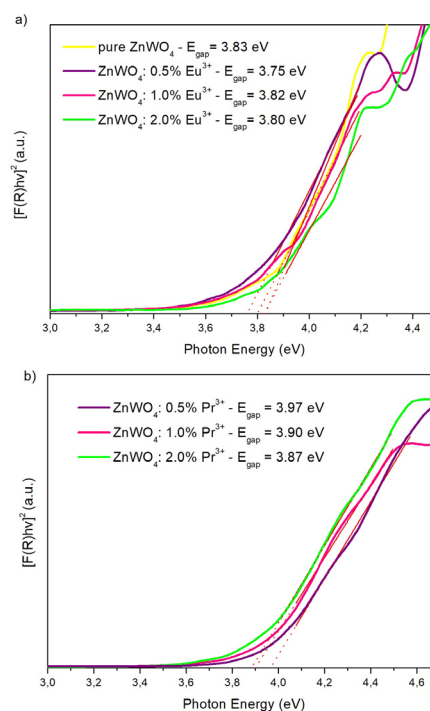


**Figure 2.** UV–Vis spectra of: a) pure and  $\text{ZnWO}_4: \text{Eu}^{3+}$  b)  $\text{ZnWO}_4: \text{Pr}^{3+}$ .

FT-IR spectra of the  $\text{RE}^{3+}$ -doped  $\text{ZnWO}_4$  (Fig. 3) show the main absorption bands at 400–1050  $\text{cm}^{-1}$ . The bands at 464 and 668  $\text{cm}^{-1}$  are assigned to bending vibrations of the W–O bonds. The peaks at 705 and 815  $\text{cm}^{-1}$  correspond to stretching vibration of the W–O bonds. The Zn–O–W bond vibrations result in a peak at 880  $\text{cm}^{-1}$  owing to bending and stretching deformations. For the  $\text{ZnO}_6$  and  $\text{WO}_6$  octahedra, the symmetric and asymmetric deformation modes of the W–O and Zn–O bonds are observed at 560 and 432  $\text{cm}^{-1}$ , respectively [3].

Figures 4a–f shows TEM images of  $\text{Eu}^{3+}$ -doped  $\text{ZnWO}_4$ . This technique was used to verify the particle size, homogeneity and shape of the crystals.

For pure  $\text{ZnWO}_4$  the HR-TEM images revealed homogenous nanorods (20–40 nm in length) with grow along (021) direction. However, for  $\text{ZnWO}_4$  doped with 0.5 mol % of  $\text{Eu}^{3+}$  we have observed the presence of both nanorods and nanospheres. With the increase of dopant amount for 1.0 and 2.0 mol % of  $\text{Eu}^{3+}$ ,

respectively) has occurred a decrease crystal size and only nanospheres morphologies has been visualized. The uniform size distributions

were dependent on the  $\text{Eu}^{3+}$  doping concentration.

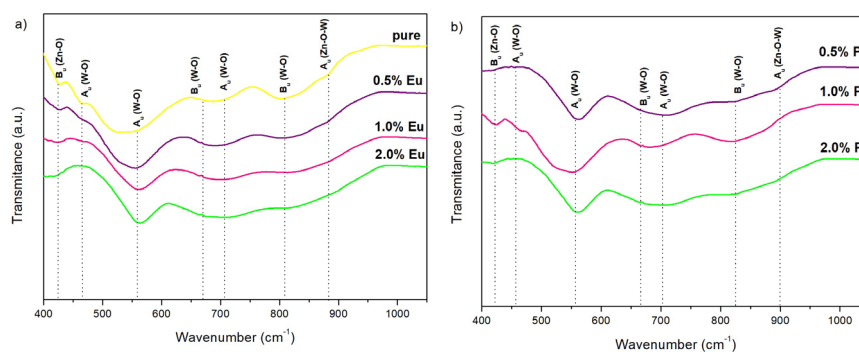


**Figure 3.** FT-IR spectra of: a)  $\text{Eu}^{3+}$ -doped and b)  $\text{Pr}^{3+}$ -doped  $\text{ZnWO}_4$ .

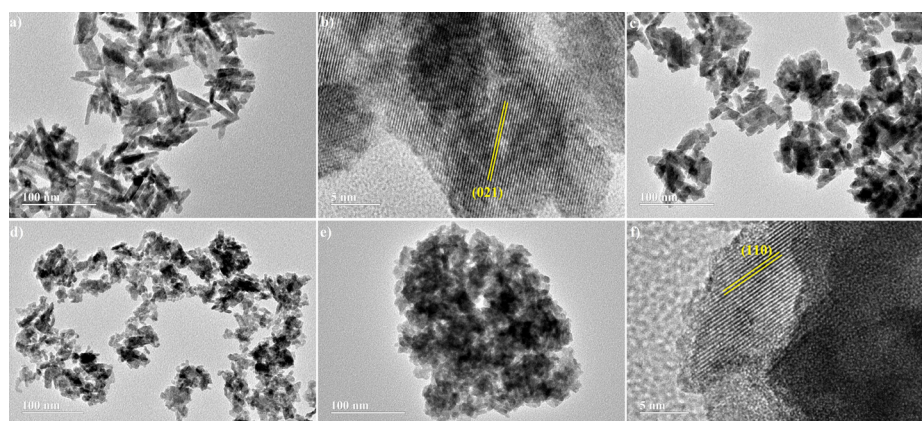


**Figure 4.** HR-TEM images of a) pure  $\text{ZnWO}_4$  b) magnified image of pure  $\text{ZnWO}_4$  c)  $\text{ZnWO}_4$ : 0.5%  $\text{Eu}^{3+}$  d)  $\text{ZnWO}_4$ : 1.0%  $\text{Eu}^{3+}$  e)  $\text{ZnWO}_4$ : 2.0%  $\text{Eu}^{3+}$  f) magnified image of  $\text{ZnWO}_4$ : 2.0%  $\text{Eu}^{3+}$ .

### 3. Material and Methods

#### Synthesis

Rare-earth doped  $\text{ZnWO}_4$  crystals (with 0.5, 1.0, and 2.0 mol% of  $\text{Eu}^{3+}$  and  $\text{Pr}^{3+}$ ) were synthesized by the coprecipitation method at room temperature followed by microwave hydrothermal method (MWH). First,  $5 \times 10^{-3}$  mol of  $\text{Na}_2\text{WO}_4 \cdot 2\text{H}_2\text{O}$  was dissolved in distilled water (50 mL). Separately,  $5 \times 10^{-3}$  mol of  $\text{Zn}(\text{NO}_3)_2 \cdot 6\text{H}_2\text{O}$  was dissolved in distilled water (50 mL) at pH 6, and the dopant of  $\text{Eu}(\text{NO}_3)_3 \cdot 5\text{H}_2\text{O}$  or  $\text{Pr}(\text{NO}_3)_3 \cdot 6\text{H}_2\text{O}$  was added to the aqueous solutions containing  $\text{Zn}^{2+}$  ions. Subsequently this solution was added to the  $\text{WO}_4^{2-}$  solution at room temperature. Finally, the white suspension formed was placed in a Teflon autoclave. The Teflon autoclave was placed inside a microwave system (2.45 GHz, power of 800 W, pressure of 245 kPa) at 140 °C for 1 h at

25 °C  $\text{min}^{-1}$ . The suspension was washed with distilled water until pH 7. The  $\text{ZnWO}_4$ :  $\text{Re}^{3+}$  were collected and dried at 60 °C for 6 h.

All the samples were characterized by X-ray powder diffraction [D/Max-2500PC diffractometer (Rigaku, Japan), with  $\text{Cu-K}\alpha$  radiation ( $\lambda = 1.5406 \text{ \AA}$ ) in the  $2\theta$  range from 10° to 70° at a scanning rate of 0.02°  $\text{min}^{-1}$ ]. The morphology and size of materials were investigated by high-resolution transmission electron microscopy (HR-TEM, Tecnai G2-F20 microscope). Ultraviolet-Visible (UV-Vis) spectra were recorded using a Varian spectrophotometer (Cary 5G, USA) in diffuse reflectance mode.

### 4. Conclusions

The insertion and variation of the rare earth dopants concentration has possibilitated the

formation of new structures as well as the change on the morphology from nanorods (for pure ZnWO<sub>4</sub> crystals) to nanospheres (for RE doped ZnWO<sub>4</sub> crystals). Consequently, the effect of the decrease in crystallite size and the creation of intermediate electronic levels enabled the decrease of E<sub>gap</sub>. These results suggest that our crystals have great potential for applications such as in phosphors, fluorescent lamps, display panels as well as photocatalysis applications and others.

## Acknowledgments

The authors appreciate the support of the Brazilian research financing institutions: CAPES/PROCAD: 2013/2998/2014; CNPq 485518/2013-9; CNPq 307054/2015-2; FAPESP CDMF 2013/07296-2.

## References and Notes

- [1] Xia, Z.; Yang, F.; Qiao, L.; Yan, F. *Opt. Commun.* **2017**, *387*, 357. [\[Crossref\]](#)
- [2] Chai, X.; Li, J.; Wang, X.; Li, Y.; Yao, X. *RSC Advanc.* **2017**, *7*, 40046. [\[Crossref\]](#)
- [3] Gonçalves, R. F.; Longo, E.; Marques, A. P. A.; Silva, M. D. P.; Cavalcante, L. S.; Nogueira, I. C.; Pinatti, I. M.; Pereira, P. F. S.; Godinho, M. *J. Mater. Sci: Mater. Electron.* **2017**, *28*, 15466. [\[Crossref\]](#)
- [4] Fang, L.; Luqiao, Y.; Ying, S.; Jianjun, X.; Lei, Z.; Lingcong, F. *J. Rare Earths* **2016**, *34*, 1179. [\[Crossref\]](#)
- [5] Chen, G.; Wang, F.; Yu, J.; Zhang, H.; Zhang, X. *J. Mol. Struct.* **2017**, *1128*, 1. [\[Crossref\]](#)
- [6] Ganiger, S. K.; Chalubaraju, B. V.; Ananda, S. R.; Murugendrapa, M. V. *Mat.Today: Proceedings* **2018**, *5*, 2803. [\[Crossref\]](#)
- [7] Kaur R.; Vellingiri, K.; Kim K-H.; Paul, A. K.; Deep, A. *Chemosphere* **2016**, *154*, 620. [\[Crossref\]](#)
- [8] Liu, Z.; Tian, J.; Zeng, D.; Yu, C.; Zhu, L.; Huang, W.; Yang, K.; Li, D. *Mat. Res. Bull.* **2017**, *94*, 298. [\[Crossref\]](#)
- [9] Luo, L.; Liu, T.; Zhang, S.; Ke, B.; Yu, L.; Hussain, S.; Lin, L. *Ceram. Int.* **2017**, *43*, 6, 5095. [\[Crossref\]](#)
- [10] Yang, Y.; Zhu, J.; Shi, W.; Zhou, J.; Gong, D.; Gu, S.; Wang, L.; Xu, Z.; Lu, B. *Mat. Lett.* **2016**, *177*, 34. [\[Crossref\]](#)
- [11] Zhan, S.; Zhou, F.; Huang, N.; He, Q.; Zhu, Y. *Chem. Eng. J.* **2017**, *330*, 635. [\[Crossref\]](#)
- [12] Zhan, S.; Zhou, F.; Huang, N.; Liu, Y.; He, Q.; Tian, Y.; Yang, Y.; Ye, F. *Appl. Surf. Sci.* **2017**, *391*, 609. [\[Crossref\]](#)
- [13] Wang, Y.; Liping, L.; Li, G. *Appl. Surf. Sci.* **2017**, *393*, 159. [\[Crossref\]](#)
- [14] Yongqing, Z.; Xuan, L.; Jia, L.; Man, J. *J. Rare Earths* **2015**, *33*, 350. [\[Crossref\]](#)
- [15] Phuruangrat, A.; Dumrongrojthanath, P.; Thongtem, T.; Thongtemi, S. *J. Ceram. Soc. Jpn.* **2017**, *125*, 62. [\[Crossref\]](#)
- [16] Peralta, M. L. R.; Sánchez-Cantú, M.; Puente-López, E.; Rubio-Rosas, E.; Tzompantzi, F. *Catal. Today* **2018**, *305*, 75. [\[Crossref\]](#)
- [17] Alam, U.; Khan, A.; Ali, D.; Bahnmann, D.; Muneer, M. *RSC Adv.* **2018**, *8*, 17582. [\[Crossref\]](#)
- [18] Kundu, S.; Ma, L.; Chen, Y.; Liang, H. *J. Photochem. Photob., A: Chemistry* **2017**, *346*, 249. [\[Crossref\]](#)
- [19] Dutta, D. P.; Raval, P. *J. Photochem. Photob., A: Chemistry* **2018**, *357*, 193. [\[Crossref\]](#)
- [20] Lu, J.; Liu, M.; Zhou, S.; Zhou, X.; Yang, Y. *Dyes Pigm.* **2017**, *136*, 1. [\[Crossref\]](#)